

Magnetic reordering in the vicinity of a ferromagnetic/antiferromagnetic interface

P. J. Jensen^{1 a}, H. Dreysse², and Miguel Kiwi³

¹ Institut für Theoretische Physik, Freie Universität Berlin, Arnimallee 14, D-14195 Berlin, Germany

² IPCMS – GEMME, Université Louis Pasteur, 23, rue du Loess, F-67037 Strasbourg, France

³ Facultad de Física, Pontificia Universidad Católica de Chile, Casilla 306, Santiago, Chile 6904411

Received: November 11, 2018/ Revised version:

Abstract. The magnetic arrangement in the vicinity of the interface between a ferromagnet and an anti-ferromagnet is investigated, in particular its dependence on the exchange couplings and the temperature. Applying a Heisenberg model, both sc(001) and fcc(001) lattices are considered and solved by a mean field approximation. Depending on the parameter values a variety of different magnetic configurations emerge. Usually the subsystem with the larger ordering temperature induces a magnetic order into the other one (magnetic proximity effect). With increasing temperature a reorientation of the magnetic sublattices is obtained. For coupled sc(001) systems both FM and AFM films are disturbed from their collinear magnetic order, hence exhibit a similar behavior. This symmetry is absent for fcc(001) films which, under certain circumstances, may exhibit two different critical temperatures. Analytical results are derived for simple bilayer systems.

PACS. 75.10.-b General theory and models of magnetic ordering – 75.25.+z Spin arrangements in magnetically ordered materials – 75.70.-i Magnetic properties of thin films, surfaces, and interfaces

1 Introduction

Magnetic reordering in the vicinity of an interface has for a long time attracted the interest of researchers. In fact, when two magnetically ordered systems are in atomic contact with each other, it is quite natural to expect that in the vicinity of the interface a novel magnetic arrangement, different from the bulk one, will set in. This phenomenon is usually referred to as the magnetic proximity effect (MPE). To the best of our knowledge this effect was first investigated to treat a ferromagnet in contact with a paramagnet [1]. Since then a vast literature on the subject has been published, of which we mention just a few examples [2].

The interest in the MPE has revived lately in relation to the exchange bias effect [3]. It occurs when a thin ferromagnetic (FM) film is deposited on an antiferromagnetic (AFM) material, resulting in a shift of the hysteresis loop from its normal (symmetric) position. If the AFM has a compensated interface ('in-plane AFM'), i.e., if the number of bonds between parallel and antiparallel spin pairs across the interface is the same, the AFM often assumes an almost orthogonal magnetization with respect to the FM magnetic direction, while the spins of the AFM interface layer adopt a canted configuration. This magnetic arrangement of the AFM is usually called spin-flop-phase,

in analogy to an AFM system in an external magnetic field [4]. The occurrence of the exchange bias effect is, in most likelihood, related to a certain amount of interface disorder [5].

When considering coupled FM-AFM systems we realized that results for fully ordered structures are scarce. In previous studies the FM film is usually treated as a system with uniform layers, i.e., the spins within a given FM layer remain strictly parallel to each other [6, 7, 8, 9]. Whereas different magnetization directions for different FM layers are considered, each layer rotates solidly. We stress that in the case of a compensated FM-AFM interface an MPE may be present also for the FM layers close to the interface. Thus the magnetic structure of each FM layer is represented, in perfect analogy to the AFM layers, by two interpenetrating sublattices with different magnetization directions. The consideration of a nonuniform intralayer magnetic structure in the FM subsystem leads to new features, which in turn are strongly dependent on the underlying lattice symmetry.

Results concerning the spin reorientation of full magnetic layers have been obtained previously for various magnetic systems but, to the best of our knowledge, caused by magnetic anisotropies [7, 8, 9]. It is important to stress that although we also incorporate anisotropy, the spin rotation in ordered FM-AFM films is mainly caused by the *isotropic* exchange interactions. Moreover, these systems

^a Corresponding author

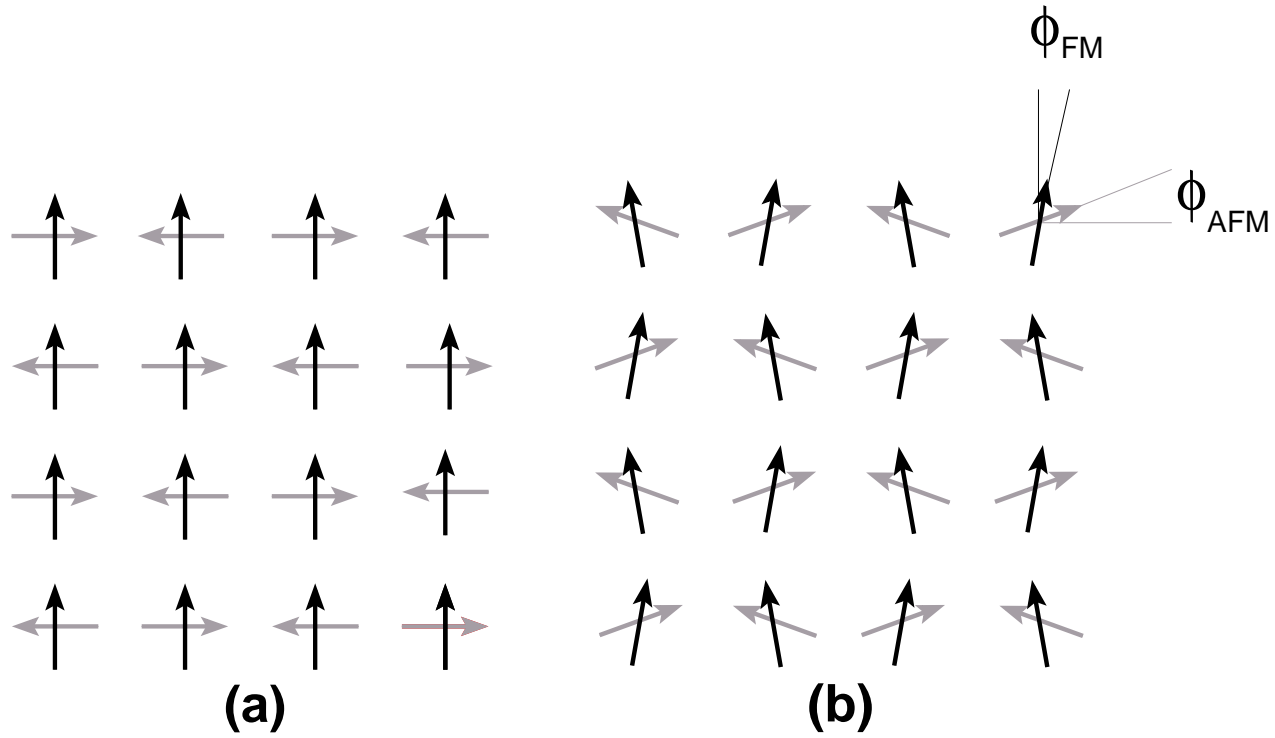


Fig. 1. Topview-sketch of the (a) decoupled ($J_{\text{int}} = 0$) and (b) coupled ($J_{\text{int}} > 0$) sc(001) bilayer system. A single FM layer (dark arrows) and a single AFM layer (grey arrows) is assumed, with two sublattices per layer. The angles ϕ_{FM} and ϕ_{AFM} quantify the deviations from the undisturbed magnetic arrangement shown in (a).

exhibit a rotation of the *magnetic sublattices*, and not a net spin reorientation of the full layers. These properties constitute an essential difference of the present treatment with respect to previous studies.

In order to derive a number of general results, while keeping the analysis as straightforward as possible, we examine at first the magnetic arrangement of a perfectly ordered bilayer consisting of a single FM layer that is coupled to a single AFM layer. Using a mean field approximation, this particular structure yields results which can be written in an *analytical form*. In addition, we present a number of results for more realistic systems having thicker FM and AFM films. In particular, we investigate the effect of the interface coupling on the characteristics and magnitude of the MPE at zero and finite temperatures. Of special concern is whether, and to which degree, magnetic order is induced by the subsystem with the higher (bare) ordering (Néel or Curie) temperature into the one with the lower ordering temperature. The resulting magnetic arrangements for various cases of the bilayer system, for films with several atomic layers, and for the corresponding ordering temperatures are determined. In fact, we show that, depending on the lattice structure, the proximity effect is not always present, and that under certain circumstances two different critical temperatures can occur.

This paper is organized as follows. In Section 2 we define our physical model. In Section 3 the magnetic prop-

erties of the bilayer system at zero temperature are discussed, which exhibits already a number of general features. Results obtained for finite temperatures are presented in Section 4. Thicker films with several FM and AFM layers are considered in Section 5. Conclusions are drawn in the last Section.

2 Theory

To model the magnetic arrangement and ordering temperatures of a coupled FM-AFM system we use an XYZ-Heisenberg Hamiltonian with localized quantum spins \mathbf{S}_i and spin number S ,

$$\mathcal{H} = -\frac{1}{2} \sum_{\langle i,j \rangle} \left(J_{ij} \mathbf{S}_i \cdot \mathbf{S}_j + D_{ij}^x S_i^x \cdot S_j^x + D_{ij}^y S_i^y \cdot S_j^y \right). \quad (1)$$

We take into account the isotropic exchange interaction J_{ij} between spins located on nearest-neighbor lattice sites i and j . In addition in-plane easy-axis exchange anisotropies D_{ij}^x and D_{ij}^y are considered, which for a particular layer are directed either along the x - or along the y -direction. Note that for two-dimensional (2D) magnets a long-range magnetic order at finite temperatures exists only in presence of such anisotropies [10]. A perfectly ordered layered structure in the xy -plane is assumed, consisting of an FM

film with n_{FM} layers and an AFM film with n_{AFM} layers. Each layer is represented by two interpenetrating sublattices, applying otherwise periodic lateral boundary conditions. The lattice symmetry, which is assumed to be the same for both FM and AFM films, is characterized by the numbers of nearest neighbors z_0 and z_1 within a layer and between adjacent layers, respectively. The latter value also refers to the number of bonds with which an FM spin is coupled across the interface to neighboring spins in the AFM layer. In this study the sc(001) and fcc(001) lattices are taken as representative and extremal examples corresponding to $z_1 = 1$ and $z_1 = 4$, respectively, and $z_0 = 4$ for both symmetries [11]. As will become apparent in the next Sections, the magnetic properties of these two types of coupled FM-AFM films differ markedly.

The FM and AFM subsystems are characterized by the exchange couplings $J_{\text{FM}} > 0$ and $J_{\text{AFM}} < 0$, and by the usually much weaker exchange anisotropies $D_{\text{FM}} > 0$ along the x -axis and $D_{\text{AFM}} < 0$ along the y -axis. Due to shape anisotropy the magnetizations of both subsystems are confined to the film plane, besides this demagnetizing effect the magnetic dipole interaction is not considered explicitly [12]. Furthermore, the FM and AFM films are coupled across the interface by the interlayer exchange coupling J_{int} , where we consider $J_{\text{int}} > 0$ without loss of generality, and $D_{\text{int}} = 0$. The (unperturbed) ground state for a small interface coupling $J_{\text{int}} \rightarrow 0$ is defined by a mutually perpendicular arrangement of the FM and AFM magnetic directions. The choice of the anisotropy easy axes support this perpendicular magnetic arrangement. A net magnetic binding results only if the spins of at least one of the subsystems are allowed to deviate from the unperturbed state. Hence, the magnetic moments cannot be represented by Ising-like spins.

In this study we apply a single-spin mean field approximation (MFA). Within this method the site-dependent magnetizations $\langle \mathbf{S}_i \rangle = \mathbf{M}_i(T)$ with components $M_i^x(T)$ and $M_i^y(T)$ are calculated, yielding the magnitudes $M_i(T) = |\mathbf{M}_i(T)|$ and in-plane angles $\tan \phi_i(T) = \pm M_i^y(T)/M_i^x(T)$. Furthermore, the ordering temperatures are determined. For decoupled monolayers ($J_{\text{int}} = 0$, $n_{\text{FM}} = n_{\text{AFM}} = 1$) the bare Curie temperature T_C^0 of the FM and the analogous Néel temperature T_N^0 of the AFM are given by

$$T_C^0 = \frac{S(S+1)}{3} z_0 (J_{\text{FM}} + D_{\text{FM}}),$$

$$T_N^0 = \frac{S(S+1)}{3} z_0 |J_{\text{AFM}} + D_{\text{AFM}}|, \quad (2)$$

where the Boltzmann constant k_B is set equal to unity. For thicker films the ordering temperature is determined by the largest eigenvalue of a particular matrix. We will investigate the MPE for a number of different cases, i.e., whether and to which degree a magnetic order propagates from the subsystem with the larger bare ordering temperature into the other one. The corresponding magnetic structure is characterized by the magnetization vectors $\mathbf{M}_i(T)$. As mentioned, at first we will consider the particularly simple bilayer system ($n_{\text{FM}} = n_{\text{AFM}} = 1$) which

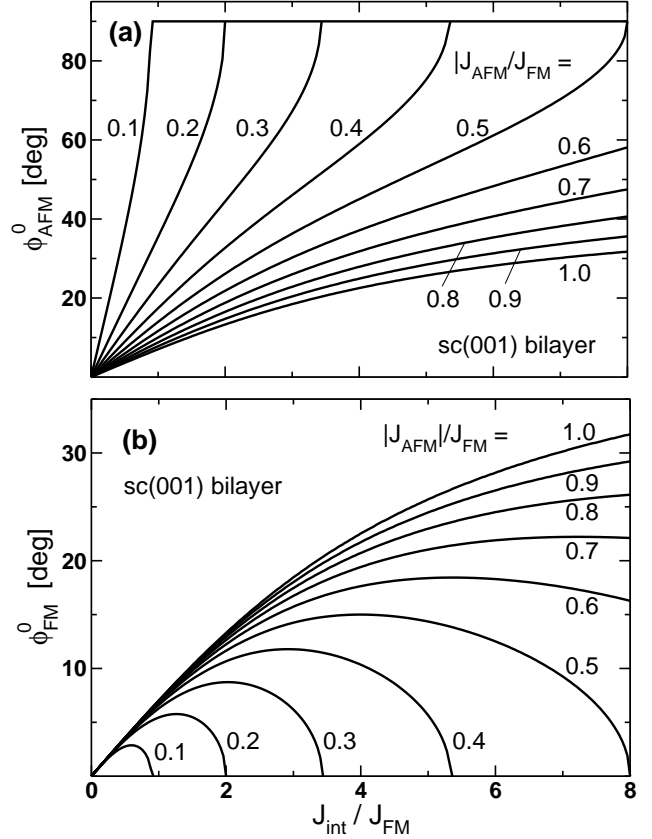


Fig. 2. Equilibrium angles (a) ϕ_{AFM}^0 of the AFM layer and (b) ϕ_{FM}^0 of the FM layer as functions of the interlayer exchange coupling J_{int} for an sc(001) bilayer at $T = 0$. The different plots correspond to different AFM exchange couplings J_{AFM} . J_{FM} is the exchange in the FM layer, and z_0 and z_1 the numbers of nearest neighbors within a layer and between adjacent layers.

allows to draw a number of general results and analytical expressions. Later on we take into account coupled FM-AFM systems with thicker films. Since the explicit consideration of anisotropies is not decisive within MFA, for simplicity we include them into the exchange couplings: $J_{\text{FM}} + D_{\text{FM}} \rightarrow J_{\text{FM}}$ and $J_{\text{AFM}} + D_{\text{AFM}} \rightarrow J_{\text{AFM}}$. For the spin quantum number we use $S = 1$ throughout.

3 Bilayers: Zero temperature

3.1 sc(001) – bilayer

For this lattice type *both* the FM and AFM layers are disturbed from their ground state, thus also the FM layer ‘dimerizes’ and exhibits a noncollinear magnetization. The undisturbed magnetic arrangement of an sc(001) bilayer is depicted in Figure 1a. For $J_{\text{int}} > 0$ both FM and AFM layers assume a canted magnetic arrangement, as sketched in Figure 1b. The canting angles ϕ_{FM} and ϕ_{AFM} represent the deviations from the decoupled bilayer.

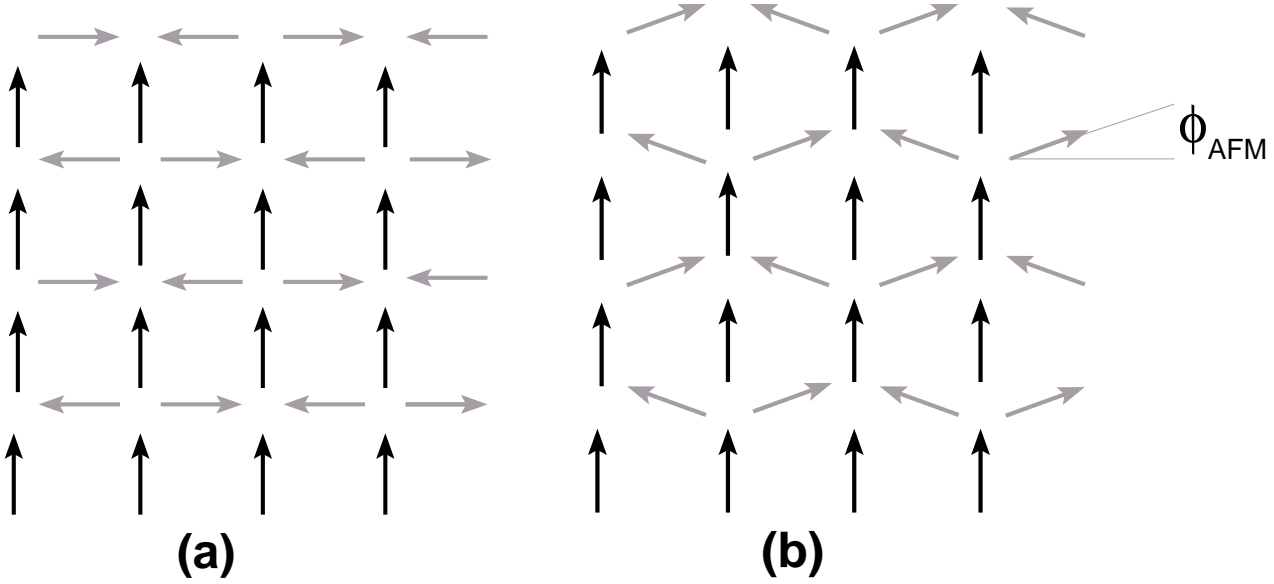


Fig. 3. Same as Figure 1 for an fcc(001) bilayer. The angle ϕ_{AFM} quantifies the deviation from the undisturbed AFM arrangement. The FM layer remains collinear.

The energy of such an arrangement is given by

$$\begin{aligned}
 E_{\text{sc}(001)}(\phi_{\text{FM}}, \phi_{\text{AFM}}) = & \\
 -\frac{z_0}{2} J_{\text{FM}} \cos(2\phi_{\text{FM}}) - \frac{z_0}{2} |J_{\text{AFM}}| \cos(2\phi_{\text{AFM}}) & \\
 -z_1 J_{\text{int}} \cos(\pi/2 - \phi_{\text{FM}} - \phi_{\text{AFM}}). & \quad (3)
 \end{aligned}$$

Differentiation of $E_{\text{sc}(001)}(\phi_{\text{FM}}, \phi_{\text{AFM}})$ with respect to ϕ_{FM} and ϕ_{AFM} yields the conditions for the equilibrium angles ϕ_{FM}^0 and ϕ_{AFM}^0 ,

$$\begin{aligned}
 z_0 J_{\text{FM}} \sin(2\phi_{\text{FM}}^0) = z_0 |J_{\text{AFM}}| \sin(2\phi_{\text{AFM}}^0) & \\
 = z_1 J_{\text{int}} \cos(\phi_{\text{FM}}^0 + \phi_{\text{AFM}}^0). & \quad (4)
 \end{aligned}$$

We emphasize that this behavior refers to a magnetic rotation of the two sublattices, with angles ϕ_i^0 and $\pi - \phi_i^0$, and not to a net spin reorientation of layer i .

First we consider $|J_{\text{AFM}}| < J_{\text{FM}}$. In Figure 2 the angles ϕ_{FM}^0 and ϕ_{AFM}^0 are shown as functions of the interlayer coupling J_{int} for different values of $|J_{\text{AFM}}|$. The following properties are quite apparent:

- For a small $|J_{\text{AFM}}|$ the AFM spins quickly turn into the direction of the FM as J_{int} increases. A parallel orientation of the AFM spins with respect to the FM, i.e., $\phi_{\text{AFM}}^0 = 90^\circ$ and $\phi_{\text{FM}}^0 = 0^\circ$, is reached at the particular strength $J_{\text{int}}^{\parallel}$ of the interlayer coupling, given by

$$J_{\text{int}}^{\parallel} = \frac{z_0}{z_1} \frac{2 J_{\text{FM}} |J_{\text{AFM}}|}{J_{\text{FM}} - |J_{\text{AFM}}|}. \quad (5)$$

The larger $|J_{\text{AFM}}|$ the larger is the value of $J_{\text{int}}^{\parallel}$ required to reach that limit.

- With increasing J_{int} the FM angle ϕ_{FM}^0 increases and exhibits a maximum at

$$J_{\text{int}}^{\text{max}} = \frac{z_0}{z_1} |J_{\text{AFM}}| \sqrt{\frac{2 J_{\text{FM}}}{J_{\text{FM}} - |J_{\text{AFM}}|}}, \quad (6)$$

assuming the value $\sin(2\phi_{\text{FM}}^{\text{max}}) = |J_{\text{AFM}}|/J_{\text{FM}}$ and coinciding with $\phi_{\text{AFM}}^0 = 45^\circ$. Notice that $\phi_{\text{FM}}^0(J_{\text{int}})$ and $\phi_{\text{AFM}}^0(J_{\text{int}})$ in general are not symmetric with respect to $J_{\text{int}}^{\text{max}}$.

- For the limiting case $|J_{\text{AFM}}| = J_{\text{FM}}$, no maximum of ϕ_{FM}^0 is obtained. Instead one has $\tan(2\phi_{\text{FM}}^0) = \tan(2\phi_{\text{AFM}}^0) = (z_1 J_{\text{int}})/(z_0 J_{\text{FM}})$. For $J_{\text{int}} \rightarrow \infty$ one obtains $\phi_{\text{FM}}^0 = \phi_{\text{AFM}}^0 = 45^\circ$.
- For $J_{\text{int}} < 0$ the same results emerge, if one performs the transformations $\phi_{\text{FM}}^0 \rightarrow -\phi_{\text{FM}}^0$ and $\phi_{\text{AFM}}^0 \rightarrow -\phi_{\text{AFM}}^0$.
- The sc(001) bilayer is characterized by an apparent symmetry between the FM and AFM layers as determined within MFA. For $J_{\text{FM}} < |J_{\text{AFM}}|$ the behavior of the FM and AFM layers, in particular the equilibrium angles ϕ_{FM}^0 and ϕ_{AFM}^0 , becomes interchanged, as can be seen from the symmetry of equations (3) and (4). If one exchanges J_{FM} and $|J_{\text{AFM}}|$ in the preceding deduction, Figure 2a is valid for ϕ_{AFM}^0 and Figure 2b for ϕ_{FM}^0 . Thus, for $J_{\text{int}} > J_{\text{int}}^{\parallel}$, antiferromagnetic order of the FM layer on top of the undisturbed AFM layer sets in. Another system exhibiting this behavior is the bcc(110) bilayer.

3.2 fcc(001) – bilayer

The fcc(001) bilayer is characterized by the fact that for an undisturbed AFM the sum of the coupling energies to

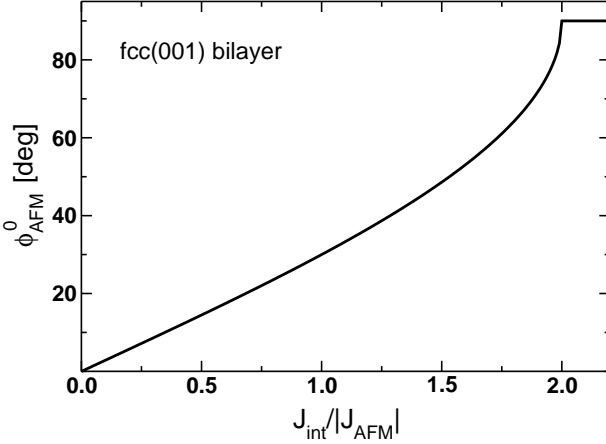


Fig. 4. Equilibrium angle ϕ_{AFM}^0 of the AFM layer as function of the interlayer exchange J_{int} for an fcc(001) bilayer at $T = 0$. The corresponding angle of the FM layer is $\phi_{\text{FM}}^0 = 0$.

a given FM spin vanishes, as can be seen from the undisturbed arrangement illustrated in Figure 3a. By setting up an equation similar to equation (3) one can show that $\phi_{\text{FM}}^0 = 0$, hence in this case the spin structure of the FM always remains strictly collinear. The resulting magnetic structure of a coupled fcc(001) bilayer is shown in Figure 3b. Thus, the symmetry between the FM and AFM subsystems of the sc(001) bilayer is no longer present for the fcc(001) one. This is a consequence of the fact that for the sc(001) bilayer each FM spin couples to a *single* AFM sublattice, while for the fcc(001) interface each FM spin couples identically to *both* AFM sublattices. A similar behavior holds for bcc(001) films.

The corresponding energy expression $E_{\text{fcc}(001)}$ is obtained from equation (3) by setting $\phi_{\text{FM}} = 0$. Differentiation with respect to ϕ_{AFM} yields the equilibrium angle ϕ_{AFM}^0 of the disturbed AFM spin arrangement,

$$\sin(\phi_{\text{AFM}}^0) = \frac{z_1 J_{\text{int}}}{2 z_0 |J_{\text{AFM}}|}, \quad (7)$$

which is shown in Figure 4 as function of J_{int} . For $z_1 J_{\text{int}} > 2 z_0 |J_{\text{AFM}}|$ one obtains $\phi_{\text{AFM}}^0 = 90^\circ$, i.e., the spins of the AFM layer order parallel to the FM ones. The case $J_{\text{int}} < 0$ is recovered by replacing $\phi_{\text{AFM}}^0 \rightarrow -\phi_{\text{AFM}}^0$.

4 Bilayer: Finite temperatures

We now turn our attention to the magnetic arrangement of the coupled FM-AFM bilayer at finite temperatures. Like in the previous Section we distinguish between an sc(001) and an fcc(001) symmetry. Furthermore, we treat the cases $T_N^0 < T_C^0$, $T_N^0 > T_C^0$, and $T_N^0 = T_C^0$ separately.

Let us at first present the ordering temperature T_C for a coupled magnetic bilayer with a collinear magnetization. Its two layers are characterized by the exchange couplings J_1 and J_2 , which can be of either sign. Within MFA one

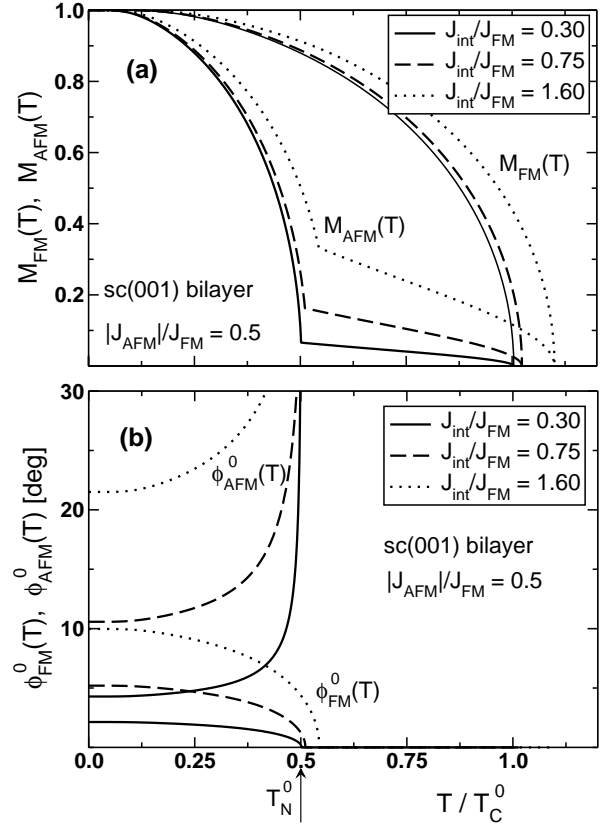


Fig. 5. (a) Magnetizations $M_i(T)$ and (b) equilibrium angles $\phi_i^0(T)$ for an sc(001) bilayer as functions of the temperature T for different values of the interlayer exchange coupling J_{int} . The AFM exchange is chosen to be $|J_{\text{AFM}}|/J_{\text{FM}} = 0.5$, hence $T_N^0 < T_C^0$. The temperature is given in units of the bare Curie temperature T_C^0 of the FM monolayer. At the sublattice reorientation temperature $T_R(J_{\text{int}}) \geq T_N^0$ one obtains $\phi_{\text{AFM}}^0(T) \rightarrow 90^\circ$ and $\phi_{\text{FM}}^0(T) \rightarrow 0$.

obtains

$$T_C = \frac{S(S+1)}{6} \left[z_0 (J_1 + J_2) + \sqrt{z_0^2 (J_1 - J_2)^2 + 4 (z_1 J_{\text{int}})^2} \right]. \quad (8)$$

Except for the cases that will be mentioned below, T_C of the coupled bilayer is always larger than the largest bare ordering temperature (T_N^0 or T_C^0) of the decoupled monolayers, regardless of the relative magnitude of J_1 and J_2 , and of the sign of J_{int} . For unequal layers ($J_1 \neq J_2$) and a small coupling J_{int} one obtains an increase of T_C given approximately by

$$\Delta T_C(J_{\text{int}}) \simeq \frac{S(S+1)}{3} \frac{(z_1 J_{\text{int}})^2}{z_0 |J_1 - J_2|}. \quad (9)$$

From the denominator of equation (9) one observes that the increase of T_C for an FM bilayer ($J_1, J_2 > 0$) will be larger than the one for a corresponding FM-AFM bilayer ($J_1 > 0, J_2 < 0$). Within MFA the results for $J_{\text{int}} < 0$

are identical to the corresponding ones for $J_{\text{int}} > 0$, if the signs of $\phi_{\text{FM}}^0(T)$ and $\phi_{\text{AFM}}^0(T)$ are adapted appropriately.

4.1 sc(001) – bilayer

a) $T_N^0 < T_C^0$. For the AFM coupling we choose $|J_{\text{AFM}}|/J_{\text{FM}} = 0.5$. In Figure 5 we display the magnetizations $M_{\text{FM}}(T)$ and $M_{\text{AFM}}(T)$, and the corresponding equilibrium angles $\phi_{\text{FM}}^0(T)$ and $\phi_{\text{AFM}}^0(T)$, as functions of the temperature T . Different values of the interlayer coupling $J_{\text{int}} > 0$ are used as indicated. At low temperatures both subsystems deviate from the undisturbed magnetic arrangement. With increasing temperature the equilibrium angle $\phi_{\text{FM}}^0(T)$ of the FM layer decreases, whereas $\phi_{\text{AFM}}^0(T)$ of the AFM layer increases. Approaching the *sublattice reorientation temperature* T_R , given implicitly by the relation

$$\begin{aligned} z_1 J_{\text{int}} [J_{\text{FM}} M_{\text{FM}}^2(T_R) - |J_{\text{AFM}}| M_{\text{AFM}}^2(T_R)] \\ = 2 z_0 J_{\text{FM}} |J_{\text{AFM}}| M_{\text{FM}}(T_R) M_{\text{AFM}}(T_R), \end{aligned} \quad (10)$$

the AFM spins turn into the direction of the FM spins, and one obtains $\phi_{\text{FM}}^0(T) \rightarrow 0^\circ$, $\phi_{\text{AFM}}^0(T) \rightarrow 90^\circ$. Thus, for $T > T_R$ the AFM layer adopts ferromagnetic order. $M_{\text{AFM}}(T)$ exhibits a sharp kink at T_R , whereas $M_{\text{FM}}(T)$ shows no particular features. The FM-AFM bilayer becomes paramagnetic above the ordering temperature T_C given by equation (8).

b) $T_N^0 > T_C^0$. Here the strength of the AFM coupling is stronger than the FM one. We adopt $|J_{\text{AFM}}|/J_{\text{FM}} = 2$ for comparison with the previous case. Then the results for $T_N^0 > T_C^0$ are fully symmetric with the ones derived for $T_N^0 < T_C^0$ shown in Figure 5, if one interchanges $M_{\text{FM}}(T) \leftrightarrow M_{\text{AFM}}(T)$, $\phi_{\text{FM}}^0(T) \leftrightarrow \phi_{\text{AFM}}^0(T)$, and $T_N^0 \leftrightarrow T_C^0$. Thus new figures are not required. Notice that for $T > T_R$ the FM layer assumes an antiferromagnetic structure. This finding demonstrates the symmetry of the FM and AFM layers of the sc(001) lattice within MFA, which also holds for finite temperatures.

c) $T_N^0 = T_C^0$. For the particular case $J_{\text{AFM}} = -J_{\text{FM}}$ the angles $\phi_{\text{FM}}^0(T)$ and $\phi_{\text{AFM}}^0(T)$ are independent of the temperature and are given by $\tan(2\phi_{\text{FM}}^0) = \tan(2\phi_{\text{AFM}}^0) = (z_1 J_{\text{int}})/(z_0 J_{\text{FM}})$. The magnetizations $M_{\text{FM}}(T)$ and $M_{\text{AFM}}(T)$ are identical and vanish at the ordering temperature, cf. equation (8),

$$T_C = \frac{S(S+1)}{3} z_0 J_{\text{FM}} \sqrt{1 + j_{\text{int}}^2}. \quad (11)$$

4.2 fcc(001) – bilayer

As mentioned in Section 3, the behavior of the fcc(001) bilayer system is not symmetric, which also holds for finite temperatures. Several cases have to be distinguished, for this purpose we define the *crossover interlayer coupling*

$$J_{\text{int}}^* = \frac{z_0}{z_1} \sqrt{2|J_{\text{AFM}}| (|J_{\text{AFM}}| - J_{\text{FM}})}. \quad (12)$$

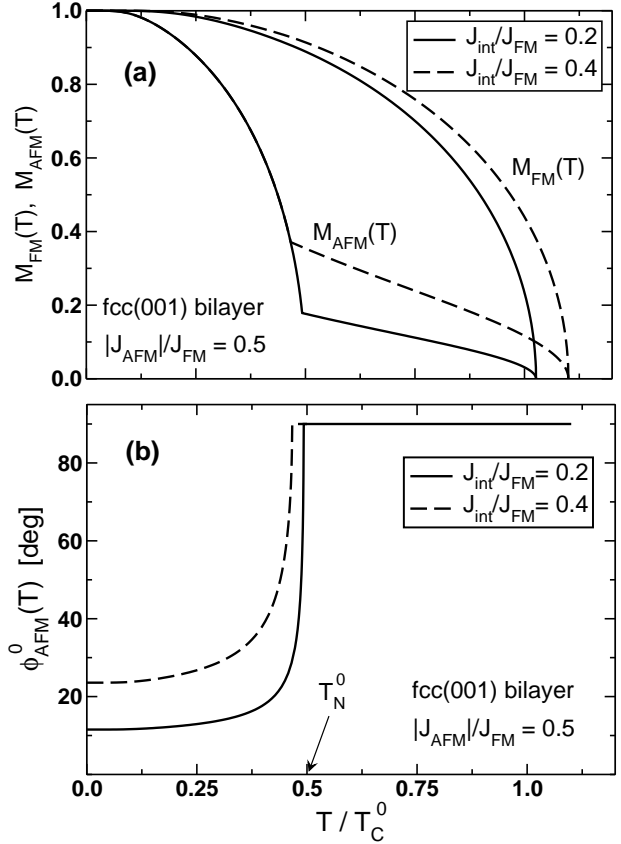


Fig. 6. (a) Magnetizations $M_i(T)$ and (b) AFM equilibrium angles $\phi_{\text{AFM}}^0(T)$ of an fcc(001) bilayer as functions of the temperature T/T_C^0 for different values of J_{int} . The AFM exchange is put equal to $|J_{\text{AFM}}|/J_{\text{FM}} = 0.5$, hence $T_N^0 < T_C^0$. The FM angle is $\phi_{\text{FM}}^0(T) = 0$.

a) $T_N^0 < T_C^0$. This case is similar to the analogous sc(001) one. However, unlike that system, for the fcc(001) bilayer the spins in the FM layer remain always collinear, i.e., $\phi_{\text{FM}}^0(T) = 0$. With increasing temperature the equilibrium angle $\phi_{\text{AFM}}^0(T)$ of the AFM layer increases and approaches 90° for the temperature T_R given by

$$z_1 J_{\text{int}} M_{\text{FM}}(T_R) = 2 z_0 |J_{\text{AFM}}| M_{\text{AFM}}(T_R). \quad (13)$$

For $T > T_R$ the AFM spins remain in a ferromagnetic structure up to the ordering temperature given by equation (8). This behavior is depicted in Figure 6 for different values of J_{int} . Notice that due to the larger number z_1 of interlayer bonds the influence of the interlayer coupling for the fcc(001) bilayer is more pronounced as compared to the sc(001) system.

b) $T_N^0 > T_C^0$ and $J_{\text{int}} > J_{\text{int}}^*$. In effect this case is similar to the preceding one, i.e., with increasing temperature the AFM spins rotate into the direction of the FM. However, although the FM exchange is weaker than the AFM exchange in this case, due to the strong interlayer coupling the FM layer *dominates* the behavior of the AFM, and results in an ordering temperature, cf. equation (8), even larger than T_N^0 . The lack of a similar mechanism for the AFM layer emphasizes the asymmetry of the two sub-

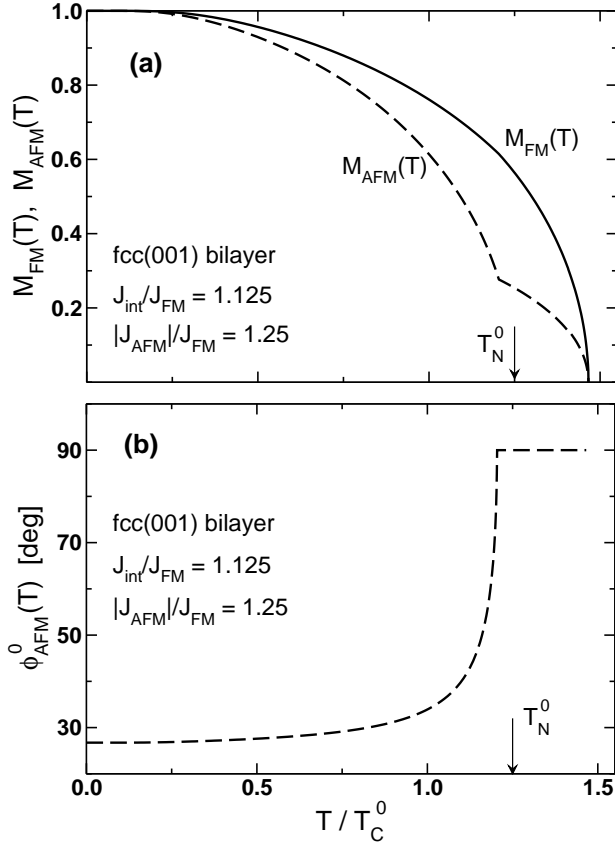


Fig. 7. Same as Figure 6 for $J_{\text{int}}/J_{\text{FM}} = 1.125$ and $|J_{\text{AFM}}|/J_{\text{FM}} = 1.25$, hence $T_N^0 > T_C^0$.

systems. Results are illustrated in Figure 7 for different values of J_{int} .

c) $T_N^0 > T_C^0$ and $J_{\text{int}} < J_{\text{int}}^*$. The asymmetric behavior of the FM and AFM layers for the fcc(001) bilayer becomes even stronger. As before, the FM layer remains collinear. However, in this case the disturbance of the AFM layer and the angle $\phi_{\text{AFM}}^0(T)$ decrease with increasing temperature, as shown in Figure 8 for different values of J_{int} . At the critical (Curie-) temperature $T_C^* > T_C^0$, given by

$$T_C^* = \frac{S(S+1)}{3} \left[z_0 J_{\text{FM}} + \frac{(z_1 J_{\text{int}})^2}{2 z_0 |J_{\text{AFM}}|} \right], \quad (14)$$

the FM layer becomes paramagnetic, although in principle coupled to a still ordered AFM layer. However, no magnetization is induced in the FM for $T > T_C^*$, since for $\phi_{\text{AFM}}^0(T) = 0$ the couplings of an FM spin across the interface to the two AFM sublattices cancel exactly, and since the scalar product of the interlayer exchange coupling, cf. equation (1), vanishes for perpendicularly oriented FM and AFM layers. The AFM layer becomes disordered at $T_C = T_N^0$, thus the bilayer ordering temperature is not given by equation (8). Evidently, in this case the interlayer exchange coupling J_{int} is not strong enough to allow the FM layer to dominate the AFM, like in the previous case. Hence, the coupled magnetic system has two critical temperatures. This behavior is present as long as

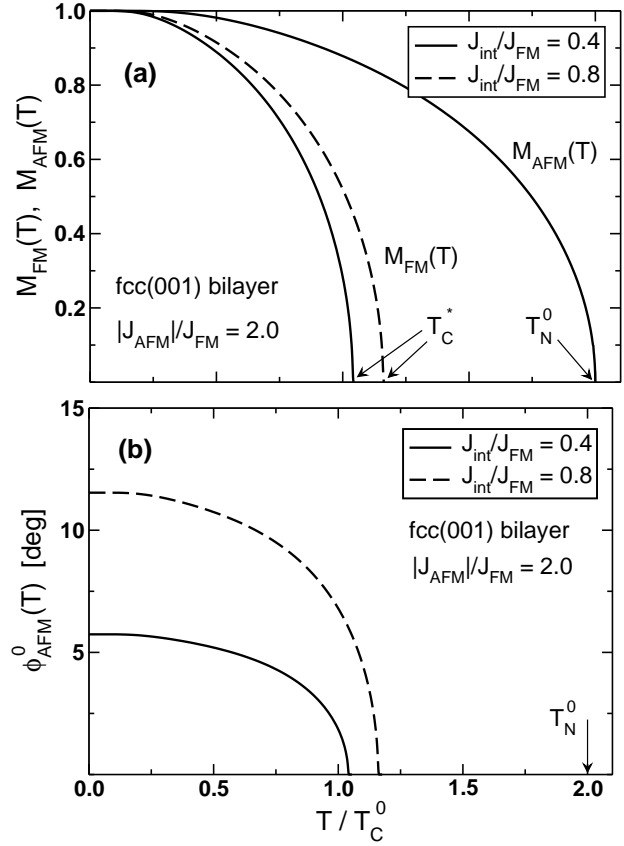


Fig. 8. Same as Figure 6 for J_{int} as indicated, and $|J_{\text{AFM}}|/J_{\text{FM}} = 2.0$, hence $T_N^0 > T_C^0$. For these systems two different critical temperatures T_C^* and T_N^0 for the FM and AFM layers, respectively, are obtained. For $T \rightarrow T_C^*$ the AFM spins relax to the undisturbed AFM arrangement.

T_C^* is smaller than T_N^0 . Equating $T_C^* = T_N^0$ yields the relation for the crossover interlayer coupling J_{int}^* given by equation (12).

5 Thicker Films

In this Section we will present a number of results for coupled FM-AFM systems, where the individual FM and AFM films are thicker than just a monolayer. Evidently, the magnetizations $M_{\text{FM}_i}(T)$ and $M_{\text{AFM}_i}(T)$, and the sublattice canting angles $\phi_{\text{FM}_i}^0(T)$ and $\phi_{\text{AFM}_i}^0(T)$ will depend on the layer i . The deviation from the undisturbed magnetic arrangement, cf. Figures 1a and 3a, is expected to be particularly pronounced for the layers close to the interface, whereas will vanish rapidly with increasing distance from the interface. In Figure 9 the equilibrium angles are shown for an sc(001) lattice symmetry at $T = 0$ as function of the AFM film thickness. For the FM film one and two layers are considered. The angles ϕ_i^0 , particularly those close to the interface, saturate within two AFM layers, while thicker AFM films exhibit a weak oscillatory behavior of decreasing amplitude which cannot be observed on the scale of the figure. An alternating sign

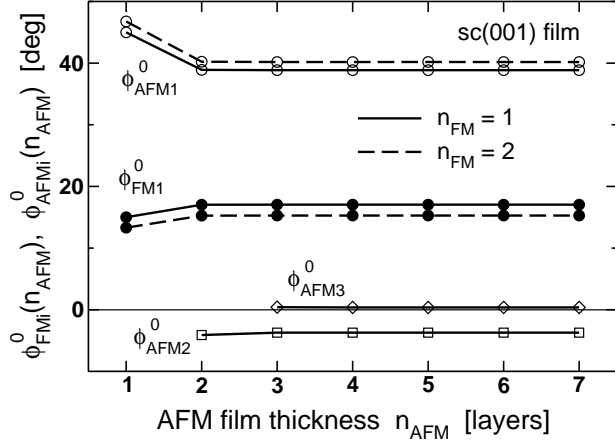


Fig. 9. Equilibrium angles ϕ_i^0 of layers i close to the interface of an sc(001) FM-AFM film as function of the AFM film thickness n_{AFM} at $T = 0$. For the couplings we assume $J_{\text{int}}/J_{\text{FM}} = 4$ and $|J_{\text{AFM}}|/J_{\text{FM}} = 0.5$, and for the FM thickness $n_{\text{FM}} = 1$ (solid lines) and $n_{\text{FM}} = 2$ (dashed lines). Shown are ϕ_i^0 of the FM interface layer (full circles), the AFM interface layer (open circles), and the subsequent two AFM layers (open squares and diamonds).

of $\phi_{\text{AFM}i}^0$ is obtained for neighboring AFM layers. For distances from the interface larger than approximately three layers the AFM remains virtually undisturbed. A corresponding behavior is obtained by varying the FM film thickness. Similar results have been reported for instance in [13].

Moreover, we also investigate sc(001) FM-AFM systems with thicker AFM films at finite temperatures. As for the bilayer, and also for thicker films and for $T_N^0 < T_C^0$, the AFM spins exhibit a rotation of the sublattice magnetization. With increasing temperature they turn into the direction of the FM film and become collinear above the sublattice reorientation temperature T_R , cf. Figure 10. The AFM magnetic arrangement for $T > T_R$ represents a ‘layered AFM structure’ consisting of ferromagnetic layers with an alternating orientation for neighboring layers. All AFM layers become collinear at the same temperature, the variation of $\phi_{\text{AFM}i}^0(T)$ is the steeper the larger the distance of layer i from the interface. A similar behavior is also obtained for FM films thicker than a monolayer. In addition, for $T_N^0 > T_C^0$ the behaviors of the FM and AFM subsystems are interchanged. Thus, the mentioned symmetry between FM and AFM films for the sc(001) symmetry, as calculated within MFA, is also present for thicker films.

The discussion of the corresponding behavior of fcc(001) FM-AFM films requires some introductory remarks. Unlike FM films, and unlike sc(001) AFM films, as calculated within MFA the Néel temperature $T_N(n_{\text{AFM}})$ of an fcc(001) AFM film with an in-plane AFM order and with nearest neighbor exchange interactions only does not increase with increasing thickness n_{AFM} . Merely, a constant $T_N(n_{\text{AFM}})$ given by the one of the monolayer ($n_{\text{AFM}} = 1$) results. Consequently, the same magnetizations $M_i(T)$, in-

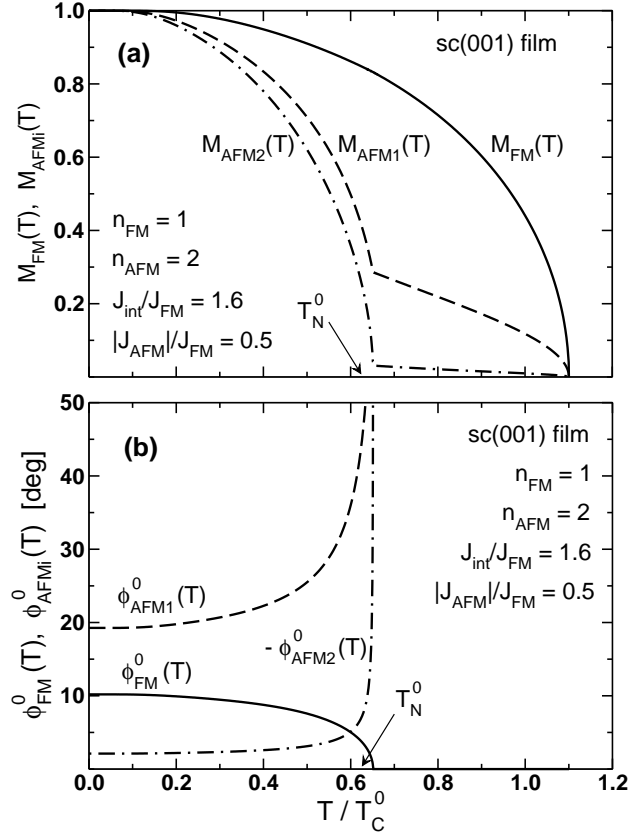


Fig. 10. (a) Magnetizations $M_i(T)$ and (b) equilibrium angles $\phi_i^0(T)$ for an sc(001) FM-AFM film as functions of the temperature T/T_C^0 . We use $n_{\text{FM}} = 1$ and $n_{\text{AFM}} = 2$, moreover, $J_{\text{int}}/J_{\text{FM}} = 1.6$ and $|J_{\text{AFM}}|/J_{\text{FM}} = 0.5$. For convenience, for the second AFM layer we show $-\phi_{\text{AFM}2}^0(T)$.

dependent of the individual layer i , are obtained. Hence, the expression for the ordering temperature, cf. equation (8), is not valid for an fcc(001) AFM bilayer. The reason is that for such a system with a collinear magnetization each layer is virtually decoupled from the rest. Only in the case of noncollinear magnetic order, as is present e.g. close to the FM-AFM interface, a net coupling between neighboring AFM layers results.

Keeping these features in mind we now discuss the finite-temperature properties of an FM-AFM system with an fcc(001) symmetry and for $n_{\text{AFM}} > 1$. As for the bilayer, all FM spins remain strictly collinear for all temperatures. In Figure 11 the magnetizations $M_i(T)$ and angles $\phi_i^0(T)$ for FM-AFM films with $n_{\text{AFM}} = 2$ and $n_{\text{AFM}} = 3$ close to their critical temperatures T_C is presented. The FM film thickness $n_{\text{FM}} = 1$ and the coupling constants are the same for both cases and are chosen in such a way that $T_N^0 > T_C^0$. The case $n_{\text{AFM}} = 2$ corresponds to the situation shown in Figure 8. The FM layer becomes paramagnetic above the critical temperature T_C^* in the presence of a still ordered AFM film. Thus, two critical temperatures can occur also for thicker FM-AFM films. The magnetizations $M_i(T)$ of the two AFM layers are identical to each other over the whole temperature range and vanish

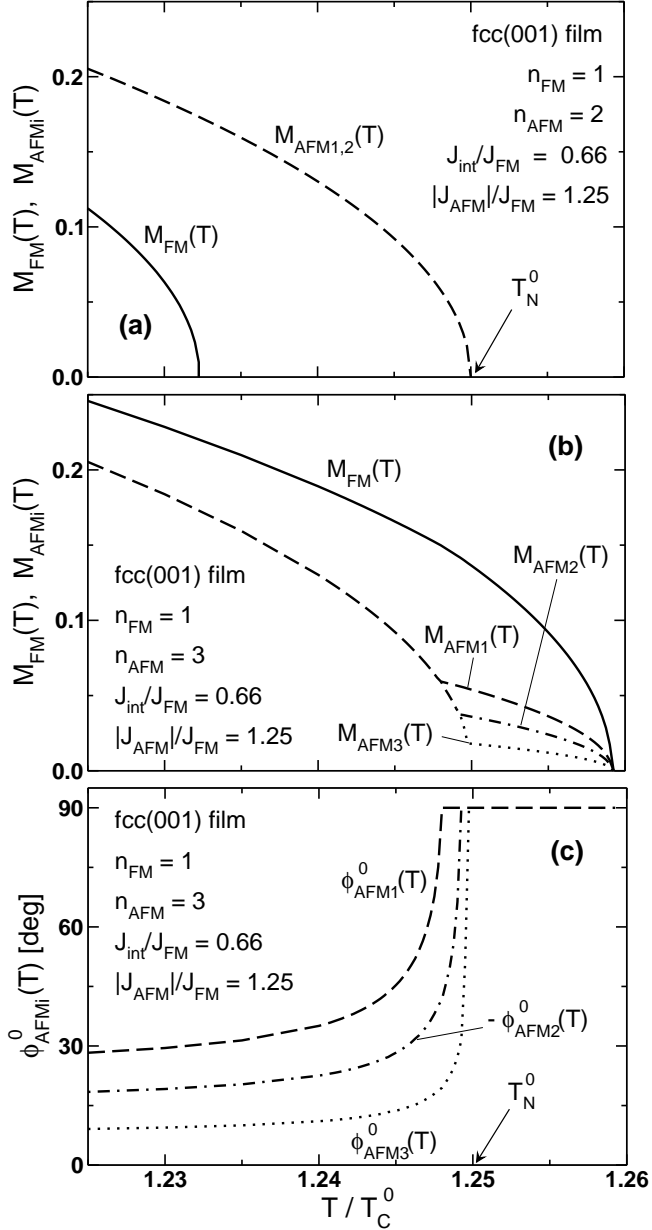


Fig. 11. Magnetizations $M_i(T)$ and equilibrium angles $\phi_i^0(T)$ for fcc(001) FM-AFM films as functions of the temperature T/T_C^0 . We have assumed a single FM layer, $J_{int}/J_{FM} = 0.66$, and $|J_{AFM}|/J_{FM} = 1.25$. (a) refers to $n_{AFM} = 2$, (b) and (c) to $n_{AFM} = 3$. For the second AFM layer $-\phi_{AFM2}^0(T)$ is depicted.

at T_N^0 ($n_{AFM} = 1$), cf. Figure 11a. In contrast, the equilibrium angles $\phi_{AFMi}^0(T)$ are different for both AFM layers, and approach $\phi_{AFMi}^0(T) \rightarrow 0$ for $T \rightarrow T_C^*$ (not shown).

For the applied coupling constants this behavior changes drastically if three AFM layers are considered. Although still $T_C^0 < T_N^0$, the FM layer now dominates and causes a similar behavior as shown in Figure 7 for an FM-AFM bilayer with a strong interlayer coupling. As can be seen from Figure 11c, the angles $\phi_{AFMi}^0(T)$ of the AFM layers increase with increasing temperature. The AFM spins eventually become collinear with respect to the FM, with

an alternating magnetic orientation for neighboring AFM layers. In contrast to the sc(001) film shown in Figure 10, the sublattice reorientation temperature $T_{R,i}$ is now layer dependent and increases as the distance of the layer i from the interface becomes larger. Moreover, as long as the AFM layers maintain a noncollinear structure, the magnetizations $M_i(T)$ are identical and independent of the layer index. Only for temperatures $T > T_{R,i}$ the $M_i(T)$ differ from each other, and vanish together with the magnetization of the FM film at the common ordering temperature T_C of the total FM-AFM system, cf. Figure 11b.

The different behavior of the AFM magnetizations in coupled sc(001) and fcc(001) FM-AFM films can be understood as follows. For the former symmetry the magnetic structures of all FM and AFM layers are disturbed for $T = 0$, and become collinear at the same temperature. On the other hand, for fcc(001) films the FM layers always remain collinear ($\phi_{FMi}^0(T) = 0$). Consider the situation depicted in Figures 11b,c. If, e.g., the spins of the AFM interface layer (AFM1) turn into the direction of the FM, the remaining AFM layers virtually experience an ordered FM film with an increased thickness. As before, the remaining AFM layers can maintain a noncollinear magnetic arrangement, and there is no need for all layers to become simultaneously collinear. In addition, we note that the AFM films above the sublattice reorientation temperatures exhibit, for both AFM thicknesses shown in Figure 11, a collinear structure. Nevertheless they behave differently since for $n_{AFM} = 2$, Figure 11a, the magnetic structure refers to an ‘in-plane AFM’ for $T > T_C^*$, and for $n_{AFM} = 3$ and $T > T_{R,i}$, Figure 11b,c, to a ‘layered AFM structure’. In the latter case the AFM magnetizations $M_i(T)$ are layer dependent, and the corresponding ordering temperature depends on the AFM film thickness.

6 Conclusion

In this study we investigated how the magnetic structure rearranges in the vicinity of the interface between a ferromagnet and an antiferromagnet. Thin film systems with sc(001) and fcc(001) symmetries have been solved for both zero and finite temperatures within the framework of a mean field approximation. A variety of configurations was obtained, and the underlying physics has been discussed. In contrast with previous work [6, 7, 8, 9], these properties are mainly determined by the isotropic exchange interactions. The consideration of a particularly simple bilayer system, and the application of an MFA at finite temperatures, allows us to derive *analytical* expressions for various quantities. These serve as estimates of the magnetic behavior for more realistic coupled FM-AFM systems having thicker FM and AFM films.

We emphasize the different behavior of the sc(001) and fcc(001) lattice symmetries. In particular, a canting of the sublattice magnetizations of both FM and AFM layers is obtained for the former case, whereas for the latter only the AFM layer is disturbed. Moreover, if the bare Curie temperature T_C^0 of the FM film is larger than the bare Néel temperature T_N^0 of the AFM film, the AFM spins become

collinear with respect to the FM system above the sublattice reorientation temperature T_R for both investigated symmetries. For $T > T_R$ the AFM film assumes a ‘layered AFM structure’. For an sc(001) lattice this reorientation happens simultaneously for all layers at the same temperature. For $T_N^0 > T_C^0$ a corresponding behavior with an interchanged role of the FM and AFM films results, which within MFA is perfectly symmetric to the case $T_N^0 < T_C^0$. In contrast, such a symmetry between FM and AFM is not present for the fcc(001) lattice. Merely, the FM spins always remain strictly collinear. The different AFM layers turn into the direction of the FM at different sublattice reorientation temperatures.

Moreover, the possibility of two critical temperatures is pointed out, as derived for fcc(001) FM-AFM bilayers for $T_N^0 > T_C^0$ and $J_{\text{int}} < J_{\text{int}}^*$. In this case the FM film becomes paramagnetic at temperatures T_C^* where the AFM film is still magnetically ordered. The presence of two different T_C ’s in magnetic systems is well known, for instance, for two coupled semi-infinite ferromagnets. Similarly, if a magnetic film with a strong exchange interaction is deposited on a bulk ferromagnet, two different ordering temperatures may exist [14]. In contrast, to our knowledge two critical temperatures for coupled magnetic films with finite thicknesses have not been reported previously.

However, the existence of two T_C ’s is expected to be fragile. In fact, small deviations from the fcc(001) symmetry, for example in presence of disorder near the interface, could destroy the lower one. The reason is that in this case the couplings of the two AFM sublattices across the interface do not cancel exactly, and a magnetization will be induced in the FM for $T > T_C^*$. In general, we note that in real FM-AFM interfaces disorder is always present, like step, vacancies, interdiffusion, etc. In this case the lateral periodicity of the magnetic structure as sketched in Figures 1b and 3b will vanish with increasing degree of disorder. The presented results are obtained for fully ordered interfaces and thus will serve as starting points to investigate the role of disorder at FM-AFM interfaces. For example, the resulting magnetic arrangement can be a mixture of the two extremal cases represented by the sc(001) and fcc(001) stackings. For a strong disorder compensated and noncompensated interfaces can no longer be distinguished [13]. Moreover, as mentioned in the Introduction, the consideration of disorder seems to be essential to explain the exchange bias effect [5].

As noted in Section 2, we have chosen anisotropy easy axes of the FM and AFM films which support a perpendicular magnetic arrangement of both subsystems. Anisotropies with different symmetries and arbitrary directions of the easy axes can be considered as well. In that case the magnetic structure and the (sublattice) spin rotation will also depend on the anisotropies. In presence of disorder the anisotropy easy axes will be site-dependent which, if the anisotropy is sufficiently strong, can disturb the lateral periodicity of the magnetic arrangements sketched in Figures 1b and 3b.

In this connection we like to point out an important difference with our prior work [9], which also dealt with

coupled FM-AFM films. There the magnetization of the FM undergoes a *full spin reorientation transition* (SRT) as a function of temperature, i.e., the net magnetization of each layer changes its direction whereas its magnitude stays approximately constant. To exhibit such an SRT a significant anisotropy in the FM must be present, eventually competing with the interlayer exchange. In contrast, in the present study both sublattices in every layer exhibit a magnetic reorientation, with opposite sense of the rotations. The directions of the net layer magnetizations remain constant and do not show an SRT, whereas their magnitudes vary considerably. These differences should become apparent in possible experimental realizations, e.g., within an element-specific X-ray magnetic linear or circular dichroism (XMLD, XMCD) measurement [15]. Whether a full SRT like in [9], or whether the magnetic arrangement as described in the present study dominates, depends on the actual FM-AFM system under consideration.

Finally, we like to discuss the influence of collective magnetic excitations (spin waves). As is well known, for 2D magnetic systems these excitations play a very important role, which however are neglected in the MFA used in this study. It is therefore important to apply improved methods which take into account collective excitations, for example, within a many-body Green’s function theory (GFT) [16]. FM-AFM bilayer and multilayer systems have been investigated previously by this method, considering a collinear magnetization [17]. In [18] the collective excitations were discussed to be a possible source for the exchange bias effect. The GFT has recently been generalized [19] to take into account several nonvanishing components of the magnetization, hence allowing the investigation of noncollinear magnetic structures. To avoid the catastrophe of the Mermin-Wagner-theorem [10] magnetic anisotropies must be incorporated explicitly. Analytical results, which can be drawn from the much simpler MFA, may not be obtained from such improved theoretical approaches. Also, it has been shown that MFA yields at least *qualitatively* correct results for anisotropic magnetic thin films, although quantitatively it strongly overestimates the ordering temperatures. Preliminary results calculated with GFT show that the main properties obtained in the present study are supported. In particular, this is valid for the sublattice magnetic reorientation, and the distortion of both FM and AFM layers in case of sc(001) FM-AFM films. On the other hand, the exact symmetry between the FM and AFM layers for the sc(001) system turns out to be an artifact of the MFA. The reason is that the spin wave dispersion relations for an FM and an AFM differ qualitatively, as do the respective ordering temperatures even for the same strengths of the exchange couplings. However, MFA incorrectly yields the same ordering temperatures. Further investigations using GFT are underway.

PJJ acknowledges support by the Deutsche Forschungsgemeinschaft through SFB 290, TP A1. HD and MK acknowledge support by ECOS. MK was also supported by Fundaci3n Andes and by FONDECYT, Chile, under grant No. 1030957.

References

1. M. J. Zuckermann, *Solid State Comm.* **12**, 745 (1973).
2. M. Kiwi and M. J. Zuckermann, *Proc. of the 19th Conf. on Magnetism and Magnetic Materials* **18**, 347 (1973); B. N. Cox, R. A. Tahir-Kheli, and R. J. Elliott, *Phys. Rev. B* **20**, 2864 (1979); G. J. Mata, E. Pestana, and M. Kiwi, *Phys. Rev. B* **26**, 3841 (1982); D. Altbir, M. Kiwi, G. Martínez, and M. J. Zuckermann, *Phys. Rev. B* **40**, 6963 (1989); J. Tersoff and L. M. Falicov, *Phys. Rev. B* **25**, R2959 (1982); *ibid.* **26**, 459, 6186 (1982); J. Mathon, M. Villeret, R. B. Muniz, J. d'Albuquerque e Castro, and D. M. Edwards, *Phys. Rev. Lett.* **74**, 3696 (1995); H. Hasegawa and F. Herman, *Phys. Rev. B* **38**, 4863 (1988).
3. For recent reviews see, e.g.: J. Nogués and I. K. Schuller, *J. Magn. Magn. Mater.* **192**, 203 (1999); M. Kiwi, *ibid.* **234/3**, 584 (2001); R. L. Stamps, *J. Phys. D: Appl. Phys.* **33**, R247 (2000).
4. L. Néel, *Ann. Phys. (Paris)* **2**, 61 (1967).
5. T. J. Moran, J. Nogués, D. Lederman, and I. K. Schuller, *Appl. Phys. Lett.* **72**, 617 (1998); M. Kiwi, J. J. Mejía-López, R. D. Portugal, and R. Ramírez, *ibid.* **75**, 3995 (1999); T. C. Schulthess and W. H. Butler, *Phys. Rev. Lett.* **81**, 4516 (1998); K. Takano, R. H. Kodama, A. E. Berkowitz, W. Cao, and G. Thomas, *ibid.* **79**, 1130 (1997); P. Miltényi, M. Gierlings, J. Keller, B. Beschoten, G. Güntherodt, U. Nowak, and K. D. Usadel, *ibid.* **84**, 4224 (2000).
6. N. C. Koon, *Phys. Rev. Lett.* **78**, 4865 (1997).
7. L. L. Hinchey and D. L. Mills, *Phys. Rev. B* **33**, 3329 (1986).
8. L. L. Hinchey and D. L. Mills, *Phys. Rev. B* **34**, 1689 (1986); N. Cramer and R. E. Camley, *ibid.* **63**, 060404(R) (2001).
9. P. J. Jensen and H. Dreyssé, *Phys. Rev. B* **66**, 220407(R) (2002).
10. N. D. Mermin and H. Wagner, *Phys. Rev. Lett.* **17**, 1133 (1966).
11. Hexagonal (111) lattice faces can also be considered appropriately. Since AFM (111) layers break up into three sublattices, the analysis will be slightly more complicated.
12. Note that for an AFM monolayer the dipole interaction prefers a perpendicular magnetization, however with a much smaller energy gain than the demagnetizing energy of an FM layer (P. J. Jensen, *Ann. Physik (Leipzig)* **6**, 317 (1997); P. Politi and M. G. Pini, *Phys. Rev. B* **66**, 214414 (2002)).
13. M. Finazzi, *Phys. Rev. B* **69**, 064405 (2004).
14. T. Kaneyoshi, I. Tamura, and E. F. Sarmiento, *Phys. Rev. B* **28**, 6491 (1983); J. M. Sanchez and J. L. Morán-López, in *Magnetic Properties of Low-dimensional systems*, edited by L. M. Falicov and J. L. Morán-López, Springer Verlag Berlin (1986), p. 114; P. J. Jensen, H. Dreyssé, and K. H. Bennemann, *Europhys. Lett.* **18**, 463 (1992).
15. A. Scholl, M. Liberati, E. Arenholz, H. Ohldag, and J. Stöhr, *Phys. Rev. Lett.* **92**, 247201 (2004).
16. S. V. Tyablikov, *Methods in the quantum theory of magnetism* (Plenum Press, New York, 1967); W. Nolting, *Quantentheorie des Magnetismus* (B. G. Teubner, Stuttgart, 1986), Vol.2.
17. H. T. Diep, *Phys. Rev. B* **40**, 4818 (1989); A. Moschel, K. D. Usadel, and A. Hucht, *Phys. Rev. B* **47**, 8676 (1993); A. Moschel and K. D. Usadel, *Phys. Rev. B* **48**, 13991 (1993).
18. H. Suhl and I. K. Schuller, *Phys. Rev. B* **58**, 258 (1998).
19. P. J. Jensen, S. Knappmann, W. Wulfhekel, and H. P. Oepen, *Phys. Rev. B* **67**, 184417 (2003); P. Fröbrich and P. J. Kuntz, *Europ. Phys. J. B* **32**, 445 (2003).